

pointing in the plus or minus directions of the ferroelectric axis. While one would expect to see a triplet in the ferroelectric and paraelectric phases, the hfs should change to a quintet in the vicinity of the Curie point. The instability of the lattice with the resulting large-amplitude protonic motion at a frequency which is still much higher than the hyperfine splitting—expressed in frequency units—should accordingly result in an averaging of the contact coupling constants over the protonic motion, so that in this region the electron would be equally coupled to all four surrounding protons.

None of these effects has been observed, and one may say that the present results support the dynamic proton order-disorder model of the ferroelectric transi-

tion in KH_2AsO_4 rather than the one involving proton displacements. The absence of such ferroelectric-mode phenomena in the proton hfs, however, does not necessarily imply that the rest of the crystal lattice does not become unstable against some collective mode as one approaches the temperature of the protonic order-disorder transition. The transition may well be an order-disorder one for hydrogens and a displacive one for the K ions.

ACKNOWLEDGMENTS

The authors are grateful to Dr. K. A. Müller and Dr. W. Berlinger for making *K*-band measurements possible, and to Dr. P. Gosar and Dr. E. A. Uehling for helpful discussions.

Energy Bands in Ferromagnetic Nickel*

JOHN W. D. CONNOLLY

Quantum Theory Project, University of Florida, Gainesville, Florida

(Received 27 February 1967)

The energy bands in ferromagnetic nickel have been calculated within the framework of the unrestricted Hartree-Fock scheme, in which the exchange terms were approximated by a local potential. The augmented-plane-wave method was used to find the eigenvalues of the approximate Hamiltonian, and self-consistency was achieved after several iterations of this method. It was found that the use of the averaged free-electron exchange potential, i.e., $\bar{V}_x^{(s)} = -6(\rho_{0s}/8\pi)^{1/3}$, gave results in qualitative disagreement with experiment. Reducing the exchange potential by a factor of $\frac{2}{3}$ gave more realistic results. Comparisons with the experimental data are presented which show that the unrestricted Hartree-Fock scheme may be an acceptable model for the ground state of a ferromagnetic solid.

I. INTRODUCTION

EXPERIMENTAL information on the metallic properties of nickel, which are dependent on the electronic configuration, has recently become available, and with it some analyses that explain these properties on the basis of the energy-band model. Energy-band models have been presented¹⁻³ which attempt to explain empirically the available data on the electronic and optical properties. Also, within the last five years, several papers have appeared in the literature⁴⁻⁸ which give the energy-band structure calculated from basic considerations, i.e., they present solutions for Schrödinger's equation in a crystal using some form of

one-electron potential. This potential, in all cases, has been derived from an atomic calculation corrected for the effects of placing the atoms in a crystalline lattice.

Although these previous calculations are qualitatively quite similar, the arbitrariness of the potential used is enough to create differences between them which are large with respect to the experimental effects which are to be explained. The calculation described in this paper attempts to eliminate this dependence on an arbitrary potential by solving the equations self-consistently, in the same way as the Hartree-Fock method used in atomic calculations. In this way, it is possible to examine the validity of the approximations which must be made in order to solve the equations.

The case of ferromagnetic nickel turns out to be extremely sensitive to slight changes in these approximations. In particular, the form in which the exchange effects responsible for the ferromagnetic structure are inserted into the theory can radically change the final results. This effect was not pointed out in previous calculations on nickel or other materials, either because the solutions were not carried to self-consistency or because the particular case was not sensitive enough to show a definite discrepancy with experiment.

* Work supported by the National Science Foundation

¹ H. Ehrenreich, H. R. Phillip, and D. J. Olechna, *Phys. Rev.* **131**, 2469 (1963).

² J. C. Phillips, *Phys. Rev.* **133**, A1020 (1964).

³ L. Hodges and H. Ehrenreich, *Phys. Letters* **16**, 204 (1965).

⁴ J. G. Hanus, Massachusetts Institute Technology Solid State and Molecular Theory Group Quarterly Progress Report No. 44, 29, 1962 (unpublished).

⁵ L. F. Mattheiss, *Phys. Rev.* **134**, A970 (1964).

⁶ E. C. Snow, J. T. Waber, and A. C. Switendick, *J. Appl. Phys.* **37**, 1342 (1966).

⁷ S. Wakoh and J. Yamashita, *J. Phys. Soc. Japan* **19**, 1342 (1964).

⁸ S. Wakoh, *J. Phys. Soc. Japan* **20**, 1894 (1965).

II. METHOD OF CALCULATION

The one-electron model for a crystal consists of the assumption that the electronic wave functions ψ_i satisfy a Schrödinger equation of the form

$$(-\nabla^2 + V(\mathbf{r}))\psi_i(\mathbf{r}) = E_i\psi_i(\mathbf{r}), \quad (1)$$

where $V(\mathbf{r})$ is a potential identical for all electrons, and includes: (i) an attractive term V_N due to the nuclei situated on the lattice sites, (ii) a repulsive term V_c due to the Coulomb interaction with the other electrons, and (iii) an attractive term V_x which simulates the exchange effects of other electrons, so that ψ_i will approximate the Hartree-Fock solution.

As a first approximation, $V(\mathbf{r})$ can be generated from the assumption that the electronic wave functions are unchanged from their atomic values. The atomic potentials on the appropriate crystalline lattice sites are then overlapped to form what has been called a "superimposed-atom potential." This, of course, makes $V(\mathbf{r})$ dependent on the particular atomic configuration chosen. Although the most logical choice would be the ground-state configuration of the atom, this is not always the best choice. It is true that the wave functions do not change greatly on going from a free atom to a crystalline environment, but the effective occupation number of each type of orbital (s , p , d , etc.) may change. The reason for this is that the discrete atomic levels which the electrons occupy in a free atom broaden into bands when these atoms come together to form a solid. If these bands happen to overlap, as they do in many metals, then electrons in one band will "spill over" into the other, thus reducing the effective number of the first type in favor of the second. This occurs in the case of nickel, in which the overlap of the $3d$ and $4s$ bands alters the configuration so that the effective number of d -like electrons is increased from the atomic ground state value of 8, to approximately 9 in the solid.

However, in a self-consistent calculation, where the potential is regenerated after each iteration, the arbitrariness in the choice of $V(\mathbf{r})$ disappears. The superimposed-atom potential is used only as a starting point for the self-consistent procedure.

For a ferromagnetic solid, the one-electron model is modified to allow $V(\mathbf{r})$ to be spin-dependent, so that the one-electron functions will approximate the unrestricted (spin-polarized) Hartree-Fock solution.^{9,10} Equation (1) then becomes two equations, one for each spin. The nuclear and Coulomb terms in these equations are straightforward, but some kind of average must be used for the exchange part of the potential. One such average, suggested by Slater,¹¹ and used with success in atomic calculations,¹² is the averaged free

⁹ J. H. Wood and G. W. Pratt, Phys. Rev. **107**, 995 (1957).
¹⁰ R. E. Watson and A. J. Freeman, Phys. Rev. **120**, 1125 (1960).

¹¹ J. C. Slater, Phys. Rev. **81**, 385 (1951).

¹² F. Herman and S. Skillman, *Atomic Structure Calculations* (Prentice-Hall, Inc., Englewood Cliffs, New Jersey, 1963).

electron exchange $\bar{V}_x^{fe} = -6(3\rho/8\pi)^{1/3}$ (in atomic units), where ρ is the local charge density. In the unrestricted case, this is generalized to

$$\bar{V}_x^{fs}, s = -6(6\rho_s/8\pi)^{1/3}, \quad (2)$$

where ρ_s is the local charge density of spin s .

Once the initial potential is chosen, the energy bands are calculated for a selected number of vectors in reciprocal space by means of the augmented-plane-wave (APW) method.¹³ This method has been sufficiently developed and checked out against other methods, so that it gives a solution (for a given potential) as accurate as desired. In its simplest form, the APW method solves Eq. (1) for a $V(\mathbf{r})$ of the "muffin-tin" type, i.e., spherically symmetric in spheres about each lattice site and constant between these spheres. This is not a necessary restriction,¹⁴ but it can be removed only at cost of much greater complexity, without much improvement in the final results.

The eigenvalues and eigenfunctions are obtained by solving a series of linear equations for each reduced vector \mathbf{k}_0

$$\sum_{\mathbf{g}'} \{ \langle \mathbf{k}_0 + \mathbf{g} | \mathcal{H} | \mathbf{k}_0 + \mathbf{g}' \rangle - E \langle \mathbf{k}_0 + \mathbf{g} | \mathbf{k}_0 + \mathbf{g}' \rangle \} c(\mathbf{k}_0 + \mathbf{g}) = 0, \\ \mathcal{H} = -\nabla^2 + V(\mathbf{r}), \quad (3)$$

where $|\mathbf{k}_0 + \mathbf{g}\rangle$ is an APW corresponding to the reciprocal lattice vector \mathbf{g} . The overlap and interaction integrals are given by the expressions

$$\langle \mathbf{k}_1 | \mathbf{k}_2 \rangle = \langle \mathbf{k}_1 | \alpha | \mathbf{k}_2 \rangle + \sum_l \langle \mathbf{k}_1 | \gamma_l | \mathbf{k}_2 \rangle I_l(E), \\ \langle \mathbf{k}_1 | \mathcal{H} | \mathbf{k}_2 \rangle = \langle \mathbf{k}_1 | \beta | \mathbf{k}_2 \rangle + \sum_l \langle \mathbf{k}_1 | \gamma_l | \mathbf{k}_2 \rangle [D_l(E) + EI_l(E)], \quad (4)$$

where

$$\langle \mathbf{k}_1 | \alpha | \mathbf{k}_2 \rangle = \Omega_0 \delta(\mathbf{k}_1, \mathbf{k}_2) - [1 - \delta(\mathbf{k}_1, \mathbf{k}_2)] \\ \times 4\pi R^2 j_1(|\mathbf{k}_1 - \mathbf{k}_2| R) / |\mathbf{k}_1 - \mathbf{k}_2|, \\ \langle \mathbf{k}_1 | \beta | \mathbf{k}_2 \rangle = \mathbf{k}_1 \cdot \mathbf{k}_2 \langle \mathbf{k}_1 | \alpha | \mathbf{k}_2 \rangle,$$

and

$$\langle \mathbf{k}_1 | \gamma_l | \mathbf{k}_2 \rangle = 4\pi(2l+1)j_l(k_1 R)j_l(k_2 R)P_l(\hat{\mathbf{k}}_1 \cdot \hat{\mathbf{k}}_2).$$

R is the radius of the spheres, Ω_0 is the volume of the unit cell outside the sphere, and

$$D_l(E) = R^2 u_l'(R, E) / u_l(R, E)$$

is the logarithmic derivative (at R) of a solution of the radial Schrödinger equation inside the sphere;

$$[ru_l(r, E)]'' + [l(l+1)/r^2 + V(r) - E][ru_l(r, E)] = 0. \quad (5)$$

¹³ J. C. Slater, Phys. Rev. **51**, 846 (1937).

¹⁴ P. D. DeCicco, Phys. Rev. **153**, 931 (1967).

The quantity $I_l(E)$ is an integral of this function, related to the logarithmic derivative,

$$I_l(E) = [u_l^2(R, E)]^{-1} \int_0^R u_l^2(r, E) r^2 dr \\ = -(\partial/\partial E) D_l(E).$$

The eigenvalues are determined by calculating the determinant

$$\det \left\| \langle \mathbf{k}_0 + \mathbf{g} | \beta - E\alpha + \sum_l D_l(E) \gamma_l | \mathbf{k}_0 + \mathbf{g}' \rangle \right\| \quad (6)$$

for a range of energies E and inverse interpolating for its zeroes.

Once the eigenvector $c(\mathbf{k}_0 + \mathbf{g})$ is determined, it is a straightforward matter to calculate the charge density corresponding to one of the zeroes of (6). The (spherically-averaged) charge density inside the sphere is

$$\bar{\rho}_{\text{in}}(r) = (4\pi N_0)^{-1} \sum_l \frac{u_l^2(r, E)}{u_l^2(R, E)} \sum_{\mathbf{g}\mathbf{g}'} c^*(\mathbf{k}_0 + \mathbf{g}) c(\mathbf{k}_0 + \mathbf{g}') \\ \times \langle \mathbf{k}_0 + \mathbf{g} | \gamma_l | \mathbf{k}_0 + \mathbf{g}' \rangle, \quad (7)$$

and the averaged (constant) charge density in the outside region is

$$\bar{\rho}_{\text{out}} = (\Omega_0 N_0)^{-1} \\ \times \sum_{\mathbf{g}\mathbf{g}'} c^*(\mathbf{k}_0 + \mathbf{g}) c(\mathbf{k}_0 + \mathbf{g}') \langle \mathbf{k}_0 + \mathbf{g} | \alpha | \mathbf{k}_0 + \mathbf{g}' \rangle. \quad (8)$$

N_0 is the normalization integral, which is expressible in terms of α , γ_l , and $I_l(E)$. The Coulomb part of a new muffin-tin potential can then be derived,^{15,16} by the method of Ewald sums, to be used in the next iteration in the self-consistent procedure,

$$V_{\text{in}}(r) = -\frac{2Z}{r} + \frac{2}{r} \int_0^r 4\pi t^2 \bar{\rho}_{\text{in}}(t) dt + 2 \int_r^R 4\pi t \bar{\rho}_{\text{in}}(t) dt, \\ V_{\text{out}} = -2\bar{\rho}_{\text{out}} \Omega_0 c/a, \quad (9)$$

where a is the lattice parameter and $c=2.41583$ is a constant characteristic of the face-centered cubic lattice.

The exchange part of the new potential is obtained by substituting the expressions (7) and (8) into Eq. (2). As in atomic calculations,¹² it was found that the use of the potential defined in (9) very often leads to a divergence in the iteration procedure. However, the scheme invented by Pratt¹⁷ (in which a new potential is interpolated from the potentials of two preceding iterations) was found sufficient to give a rapid convergence.

In practice (e.g., Ref. 18), in order to reduce the size of the determinant (6), symmetrized combinations of

¹⁵ J. C. Slater and P. D. DeCicco, Massachusetts Institute Technology Solid State and Molecular Theory Group Quarterly Report No. 50, 46, 1963 (unpublished).

¹⁶ J. W. D. Connolly, University of Florida Quantum Theory Project Technical Report No. 94, 1966 (unpublished).

¹⁷ G. W. Pratt, Phys. Rev. **88**, 1217 (1952).

¹⁸ J. H. Wood, Phys. Rev. **126**, 517 (1962).

APW's are used as basis functions, i.e., instead of taking matrix elements between $|\mathbf{k}_0 + \mathbf{g}\rangle$ in Eq. (3), we take them between functions of the type

$$|\mathbf{k}_0 + \mathbf{g} P I J\rangle = \Theta_{IJ}^P |\mathbf{k}_0 + \mathbf{g}\rangle,$$

where Θ_{IJ}^P is the standard "symmetrizing" operator

$$\Theta_{IJ}^P = (|G_0|/n_P) \sum_{\mathcal{R} \in G_0} \Gamma_P^*(\mathcal{R})_{IJ} \mathcal{R}.$$

$|G_0|$ is the order of the group G_0 of the vector \mathbf{k}_0 . The function as defined here will belong to the I th row of the P th representation of G_0 (dimension n_P). $\Gamma_P(\mathcal{R})_{IJ}$ is the (I, J) element for the P th representation corresponding to the element $\mathcal{R} \in G_0$. The matrix elements (of any operator A which commutes with G_0 , such as α , β , and γ_l) between two symmetrized APW's can be related to those between the unsymmetrized functions by the equation

$$\langle \mathbf{k}_1 P I J | A | \mathbf{k}_2 P' I' J' \rangle \\ = \delta_{PP'} \delta_{II'} \langle \mathbf{k}_1 | A | \mathbf{k}_2 P J J' \rangle \\ = (|G_0|/n_P) \delta_{PP'} \delta_{II'} \sum_{\mathcal{R} \in G_0} \Gamma_P^*(\mathcal{R})_{IJ} \langle \mathbf{k}_1 | A | \mathcal{R} \mathbf{k}_2 \rangle, \quad (10)$$

where $|\mathcal{R} \mathbf{k}\rangle$ is an unsymmetrized APW corresponding to the wave vector obtained when the group element \mathcal{R} operates on \mathbf{k} . The Kronecker deltas occurring in (10) have the effect of block-diagonalizing the determinant (6) if G_0 contains more than one element. The problem then reduces to finding the zeroes of the determinant,

$$\det \left\| \langle \mathbf{k}_0 + \mathbf{g} | \beta - E\alpha + \sum_l D_l(E) \gamma_l | \mathbf{k}_0 + \mathbf{g}' P J J' \rangle \right\|$$

for each representation P of G_0 . Care must be taken to insure that the set of (\mathbf{g}, J) are chosen so that the functions $|\mathbf{k}_0 + \mathbf{g} P I J\rangle$ are linearly-independent. Methods for this choice are given in Refs. 16 and 19.

The expressions for the charge density are the same as in Eqs. (7) and (8) with the α and γ matrix elements replaced by their symmetrized forms as given in (10).

III. RESULTS OF THE CALCULATION

A. The Self-Consistent Spin-Dependent Energy Bands

The energy eigenvalues were calculated and computed self-consistently for two values of the exchange potential: (i) the averaged free-electron value $\bar{V}_x^{\text{fe}} = -6(6\rho_s/8\pi)^{1/3}$ and (ii) the value suggested by Kohn and Sham²⁰ $= \frac{2}{3} \bar{V}_x^{\text{fe}}$. The initial potential was chosen to be a superimposed atom potential generated from unrestricted self-consistent atomic orbitals corresponding to the configuration

$$(3d\alpha)^{5.0} (3d\beta)^{4.4} (4s\alpha)^{0.3} (4s\beta)^{0.3}$$

(denoted by V_1). The value of the lattice parameter

¹⁹ A. W. Luehrmann Advan. Phys. (to be published); Ph.D. thesis, University of Chicago, 1966 (unpublished).

²⁰ W. Kohn and L. J. Sham, Phys. Rev. **140**, A1133 (1965).

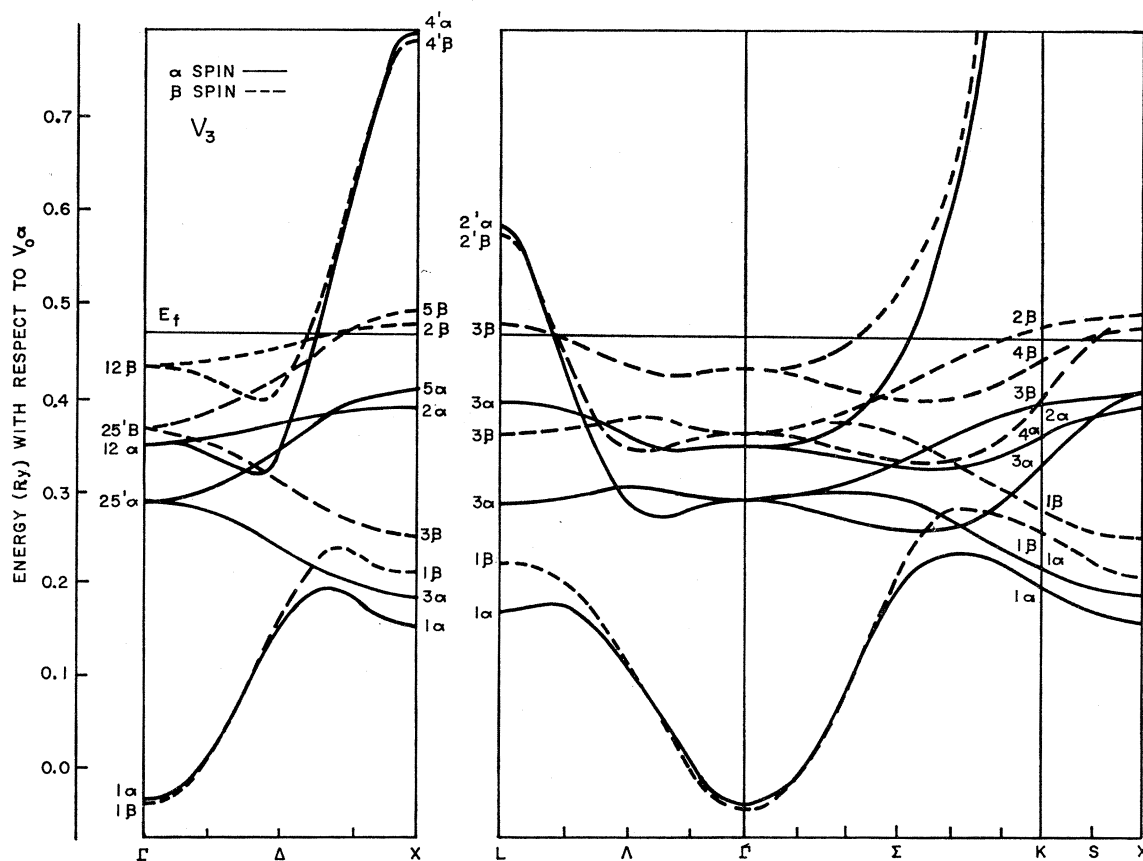


FIG. 1. The self-consistent energy bands for $V_3(V_x = \bar{V}_x^{fe})$ along the three principal symmetry direction in reciprocal space.

used was the one quoted by Wyckoff,²¹ i.e., $a = 6.6586$ atomic units. The summations over l in the matrix elements in the secular equations were taken up to a value of $l_{\max} = 6$ and the maximum reciprocal vector magnitude was $K_{\max} = 6\pi/a$. By calculating the energy eigenvalues at a few points for larger values of these parameters, it was found that the chosen values of l_{\max} and K_{\max} were sufficient to insure a convergence of less than 0.005 Ry. The d -like states tended to converge more slowly than the s - and p -like states. This is because of the large negative value of the logarithmic derivative for $l=2$, which forces a large discontinuity in the derivative of the wave function at the sphere radius. Thus, more basis functions are necessary to smooth out the d -like wave functions.

The eigenvalues and the corresponding wave functions were calculated at the 32 points of a cubic mesh in reciprocal space (Grid 1 of Table I) during the course of each iteration. Because of symmetry, actually only 6 points were calculated, and the charge densities were multiplied by the appropriate weights to derive the total charge density. For the last two iterations of both calculations, the mesh was reduced to half the former size, for an equivalent of 256 points (Grid 2 of Table I). It was found that 6 or 7 iterations were sufficient to achieve a convergence of the energy levels

to within 0.01 Ry. More accuracy was deemed unnecessary, because of the uncertainties in the one-electron potential and the approximations inherent in the muffin-tin form of this potential.

TABLE I. Coordinate grids in reciprocal space. Only the first two are listed here. Grids Nos. 3, 4, and 5 are similarly defined, having 89, 505, and 3345 nonequivalent points, respectively, and 2048, 16384, and 131072 total points in the Brillouin zone.

Grid No. 1 (6 nonequivalent points, 32 total points)					
$(a/\pi) \cdot \mathbf{k}$	Symmetry ^a	Weight	$(a/\pi) \cdot \mathbf{k}$	Symmetry	Weight
0 0 0	Γ	1	0 1 1	Σ	12
0 0 1	Δ	6	0 1 2	W	6
0 0 2	X	3	1 1 1	L	4
Grid No. 2 (20 nonequivalent points, 256 total points)					
$(2a/\pi) \cdot \mathbf{k}$	Symmetry	Weight	$(2a/\pi) \cdot \mathbf{k}$	Symmetry	Weight
0 0 0	Γ	1	0 2 3		24
0 0 1	Δ	6	0 2 4	W	6
0 0 2	Δ	6	0 3 3	K	6
0 0 3	Δ	6	1 1 1	Λ	8
0 0 4	X	3	1 1 2		24
0 1 1	Σ	12	1 1 3		24
0 1 2		24	1 1 4	U	6
0 1 3		24	1 2 2		24
0 1 4	Z	12	1 2 3	Q	24
0 2 2	Σ	12	2 2 2	L	4

²¹ R. W. G. Wyckoff, *Crystal Structures* (John Wiley & Sons, Inc., New York, 1963), Vol. I.

^a The symmetry symbols are those of L. P. Bouckaert, R. Smoluchowski, and E. Wigner, *Phys. Rev.* **50**, 58 (1936).

TABLE II. Comparison of energy differences for various potentials.

Potential	<i>d-s</i> separation		<i>d</i> width	<i>s-p</i> width	splittings	
	$\Gamma_{25'} - \Gamma_1$	$X_5 - \Gamma_1$	$X_5 - X_1$	$X_4' - \Gamma_1$	$\Delta\Gamma_{25'}$	$\Delta\Gamma_1$
$V_1\alpha^a$	0.481 ^f	0.627	0.320	0.837	0.070	0.016
$V_1\beta$	0.537	0.687	0.349	0.838		
$V_2\alpha^b$	0.437	0.571	0.299	0.836	0.070	0.013
$V_2\beta$	0.491	0.633	0.325	0.837		
$V_3\alpha^c$	0.322	0.441	0.251	0.833	0.076	-0.005
$V_3\beta$	0.403	0.531	0.282	0.834		
$V_4\alpha^d$	0.478	0.625	0.330	0.841	0.060	-0.004
$V_4\beta$	0.542	0.698	0.362	0.842		
$V_5\alpha^e$	0.488	0.639	0.347	0.865	0.067	0.018
$V_5\beta$	0.535	0.695	0.372	0.866		

^a V_1 = a superimposed-atom potential (non-self-consistent) with $V_x = \bar{V}_x^{fe}$, corresponding to the atomic configuration ($3d\alpha = 5.0$, $3d\beta = 4.4$, $4s\alpha = 4s\beta = 0.3$).

^b V_2 = a superimposed-atom potential (non-self-consistent) $V_x = \bar{V}_x^{fe}$, corresponding to the atomic configuration ($3d\alpha = 4.8$, $3d\beta = 4.2$, $4s\alpha = 4s\beta = 0.5$).

^c V_3 = the self-consistent potential with $V_x = \bar{V}_x^{fe}$.

^d V_4 = the self-consistent potential with $V_x = (2/3)\bar{V}_x^{fe}$.

^e V_5 = Wakoh's potential of Ref. 8.

^f The energy differences are given in rydbergs.

In each iteration, after the energies were computed, the Fermi energy E_f was estimated by counting the states of both spins in order of increasing energy until 10 bands were filled. Because of this procedure, the configuration (i.e., the number of *s*-, *p*-, and *d*-like states) can change from iteration to iteration, unlike the

usual atomic self-consistent calculation, in which the configuration is held fixed. This might be expected to lead to a "collapse" of the β bands on to the α bands (or perhaps a divergence, as found by Switendick²² for chromium).

In the course of the calculation, it was found that

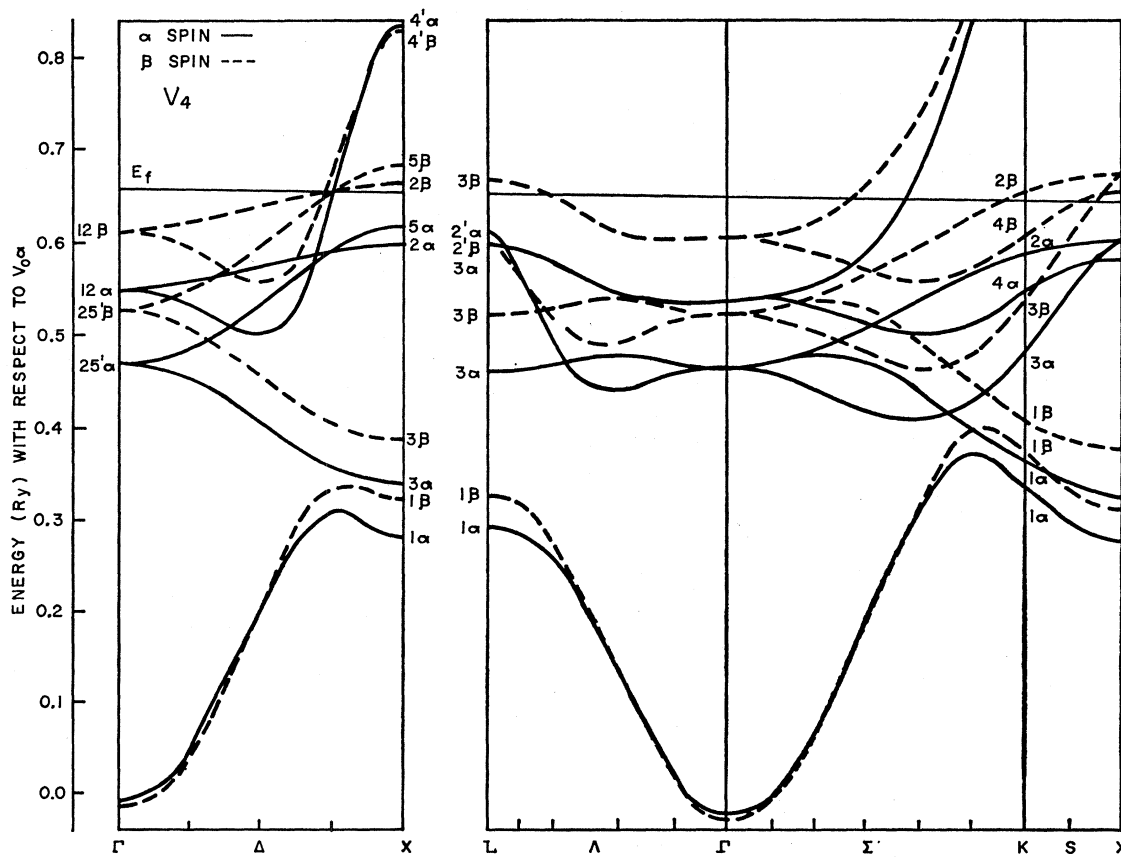


FIG. 2. The self-consistent energy bands for V_4 ($V_x = \frac{2}{3}\bar{V}_x^{fe}$) along the three principal symmetry directions in reciprocal space.

²² A. C. Switendick, J. Appl. Phys. 37, 1022 (1966).

TABLE III. Parameters used in the interpolation procedure. The units of all parameters are in rydbergs, except α (dimensionless) and B_1 (atomic units of length).

T.B.A. d -function parameters ^a	$V_3\alpha$	$V_3\beta$	$V_4\alpha$	$V_4\beta$
$E_{xy,xy}(0, 0, 0)$	0.325	0.402	0.518	0.580
$E_{\delta x^2-r^2, \delta x^2-r^2}(0, 0, 0)$	0.319	0.395	0.511	0.570
$E_{xy,xy}(1, 1, 0)$	-0.0212	-0.0232	-0.0263	-0.0282
$E_{xy,xy}(0, 1, 1)$	0.0048	0.0055	0.0058	0.0062
$E_{xy,xy}(0, 1, 1)$	0.0063	0.0074	0.0076	0.0083
$E_{x^2-y^2, x^2-y^2}(1, 1, 0)$	0.0125	0.0138	0.0154	0.0177
$E_{\delta x^2-r^2, \delta x^2-r^2}(1, 1, 0)$	-0.0078	-0.0085	-0.0096	-0.0104
$E_{xy, \delta x^2-r^2}(1, 1, 0)$	0.0111	0.0126	0.0147	0.0157
O.P.W. parameters ^{b,c}				
α	1.000	1.000	1.000	1.000
β	-0.037	-0.042	-0.009	-0.012
V_{111}	0.131	0.133	0.128	0.129
V_{200}	0.167	0.166	0.159	0.158
Hybridization parameters ^{b,d}				
B_1 ($\pi/4a$)	0.416	0.423	0.419	0.424
B_2	1.050	1.128	1.240	1.262
B_3	1.227	1.254	1.375	1.433

^a Notation of Ref. 25.^b Notation of Ref. 23.^c These parameters were kept fixed during the least squares fitting pro-cedure, so that the conduction-band effective mass was 1.0, and the conduction states Γ_1 , L_2' , and X_4' had their calculated values.^d In Ref. 23, B_2 and B_3 were assumed equal.

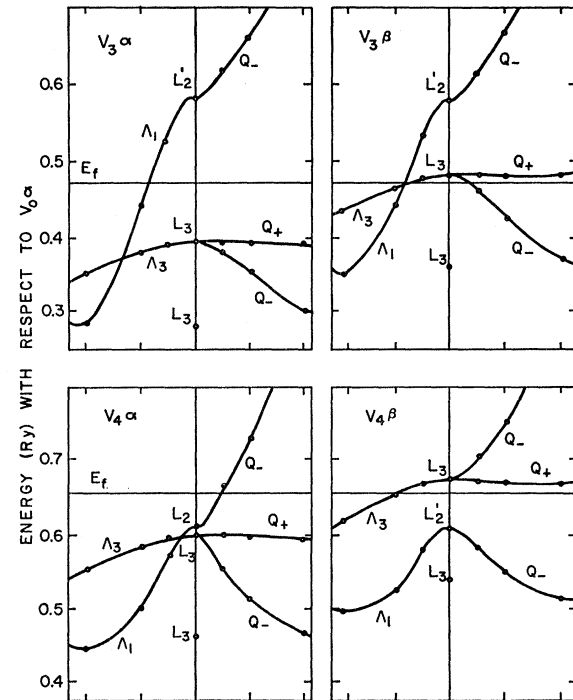
the difference between the number of electrons of either spin *did* decrease slightly, but leveled off at a constant value. This may be a fortuitous result of using a finite number of points in the Brillouin zone to calculate the density, but the fact that this constant value is close to the experimental is encouraging.

The calculation was carried out on an IBM 709 computer. The time taken per iteration was approximately one hour for Grid 1 (32 points in the Brillouin zone) and three hours for Grid 2 (256 points in the Brillouin zone).

Figure 1 shows the final bands for the first calculation (denoted by V_3) in which the exchange was chosen to have the averaged free-electron value \bar{V}_x^{fe} . Here, Δ is the $[100]$ direction, Λ is the $[111]$ direction, and Σ is the $[110]$ direction in reciprocal space. Figure 2 shows the same information for the second calculation (denoted by V_4), for which the exchange potential was taken to be $\frac{2}{3}\bar{V}_x^{fe}$. Both sets of bands have the same general shape, which is essentially determined by the symmetry of the face-centered cubic lattice. Both show the feature, typical of the transition metals, of a narrow (~ 0.3 Ry) d band imbedded in a much broader conduction band. The splitting between the two spin bands is not uniform throughout the zone, but is approximately 0.07 Ry for the d -like states and -0.005 Ry for the conduction states. The principal difference between the two sets of results is in the width and position of the d bands. These are considerably wider ($\sim 30\%$) and higher (~ 0.15 Ry) with respect to the conduction band for V_4 than for V_3 . The reason for this is that reducing the exchange effects elevates the potential by an amount proportional to $\rho^{1/3}$. Therefore, the energies of the d -like electrons, which are confined to the higher-density interior of the atom, are raised

more than the energies of the conduction electrons, which are found further out where the density is less. This elevation of the d bands tends to spread out the wave functions, thus increasing the band width. A detailed comparison of the calculated energy bands is shown in Table II.

Although the general shape of the bands is quite

FIG. 3. Detail of the energy bands in the region of the L point ($\pi/a, \pi/a, \pi/a$) for the two self-consistent potentials.

similar, the change in the position of the d bands with respect to the conduction band is sufficient to alter some of the details. For example, at the L point $(\pi/a, \pi/a, \pi/a)$ there are two doubly degenerate d -like levels L_3 , and two singly degenerate levels: L_1 (a mixture of s and d -like states) and L_2' (which has p -like symmetry). Figure 3 shows the bands in the region around this point. Λ is the line from $\Gamma(0, 0, 0)$ to L , and Q is the line perpendicular to Λ on the face of the zone, going from L to $W(\pi/a, 2\pi/a, 0)$. It can be seen from this figure that the energy bands are substantially different in the two cases, the p -like level L_2' being much lower with respect to the d bands for V_4 than for V_3 . This is particularly significant in that the position of the Fermi level with respect to the conduction band, and consequently the Fermi surfaces, are considerably altered by the shifting of the L_2' level. In particular, the Fermi surface for the α electrons is closed for V_3 and multiply connected for V_4 .

As is usual in an energy-band calculation, the eigenvalues were computed at only a few points. However, for many applications it is necessary to know the bands throughout the Brillouin zone, so that some sort of interpolation procedure is required. It has been shown²³ that a good fit to the band structure of transition metals can be obtained if the one-electron wave functions are assumed to be a linear combination of tight-binding-approximation (TBA) functions and orthogonalized plane waves (OPW), and the interaction integrals are treated as adjustable parameters. In this scheme, the energy bands are the eigenvalues of a matrix of the type

$$\begin{bmatrix} \mathcal{H}_{\text{OPW}} & \mathcal{H}_{\text{HYB}} \\ \mathcal{H}_{\text{HYB}}^\dagger & \mathcal{H}_{\text{TBA}} \end{bmatrix},$$

where \mathcal{H}_{OPW} is a 4×4 matrix of the type derived by Harrison,²⁴ \mathcal{H}_{TBA} is a 5×5 matrix whose elements are those for a d band in a fcc structure as given by Slater and Koster²⁵ and \mathcal{H}_{HYB} is a hybridization (HYB) matrix derived by Hodges *et al.*²³ which approximates the interaction between the 4 OPW's and the 5 TBA d functions.

The self-consistent energy bands V_3 and V_4 were fitted to this scheme by a least-squares procedure until the rms deviation of the interpolated values from the calculated values was less than 0.005 Ry. The resultant parameters are shown in Table III. These parameters were then used to calculate the density of states, the Fermi surfaces, and the effective masses for both potentials in order to compare the results with the experimental data.

B. Comparison with Previous Calculations

The literature of the past few years contains several calculations of the energy-band structure of nickel. The

augmented-plane-wave method has been applied to the paramagnetic case by (i) Hanus,⁴ who used a potential generated from renormalized atomic orbitals of the atomic configuration $(3d)^8(4s)^2$, (ii) Mattheiss,⁵ who used a superimposed-atom potential corresponding to $(3d)^9(4s)$, and (iii) Snow, Waber, and Switendick,⁶ who tried several different superimposed-atom potentials with atomic configurations $(3d)^{10-x}(4s)^x$, $0 \leq x \leq 2$. These three calculations are qualitatively similar to each other, differing only in the position and width of the d bands. Calculation (iii) shows, as confirmed in this work, that the d -band shift has a profound effect on the topology of the Fermi surface, caused by the altered ordering of the L -point levels. Yamashita and Wakoh^{7,8} have also done several calculations for nickel, both in the paramagnetic and ferromagnetic states, using the Green's-function method. Since this method is formally equivalent to the APW method,²⁶ their results are also very similar, showing the same sensitivity of the d bands to changes in the potential.

In order to compare all of these results, we note that each calculation can be fairly well described by only two parameters: (i) the position of the d bands with respect to the conduction band, a measure of which is the energy difference between the states Γ_{25}' and Γ_1 , and (ii) the d -band width, characterized by the energy difference between X_5 and X_1 .

Using these two parameters as coordinates, each calculation is plotted on the graph in Fig. 4. For comparison, a few calculations for other elements (Cu, Co, Fe) with an fcc structure are included.²⁷⁻³⁰ We note that no matter what the potential, all the calculations tend to lie on a straight line, which suggests that the energy-band structure of an fcc transition metal could be described by a single parameter, say, the position of the d bands.

This diagram shows clearly the considerable variation between the results of previous work. The principal differences can be traced back to the atomic configuration used. Those calculations which assumed a smaller number of d electrons are found toward the lower left-hand corner of the diagram. Although all of the calculations listed here used the averaged free-electron exchange potential \bar{V}_x^{fe} , the effect of reducing the exchange moves the results in the opposite direction. In short, anything which makes the potential more attractive for the d electrons narrows the d band and lowers it with respect to the s - p band.

Of the previous calculations on transition elements, only two have been carried to self-consistency, viz., that of Wakoh⁸ on copper and ferromagnetic nickel, and that of Snow and Waber²⁷ on copper, both of which used \bar{V}_x^{fe} . We can see by looking at Fig. 4 that there is a considerable difference between the two results for Cu (Refs. 8 and 27). Wakoh's d bands are displaced

²³ L. Hodges, H. Ehrenreich, and N. D. Lang, Phys. Rev. **152**, 505 (1966).

²⁴ W. A. Harrison, Phys. Rev. **118**, 1182 (1960).

²⁵ J. C. Slater and G. Koster, Phys. Rev. **94**, 1498 (1954).

²⁶ K. H. Johnson, Phys. Rev. **150**, 429 (1966).

²⁷ E. C. Snow and J. T. Waber, Phys. Rev. (to be published).

²⁸ B. Segall, Phys. Rev. **125**, 109 (1962).

²⁹ G. A. Burdick, Phys. Rev. **129**, 138 (1963).

³⁰ F. J. Arlinghaus, Phys. Rev. **153**, 743 (1967).

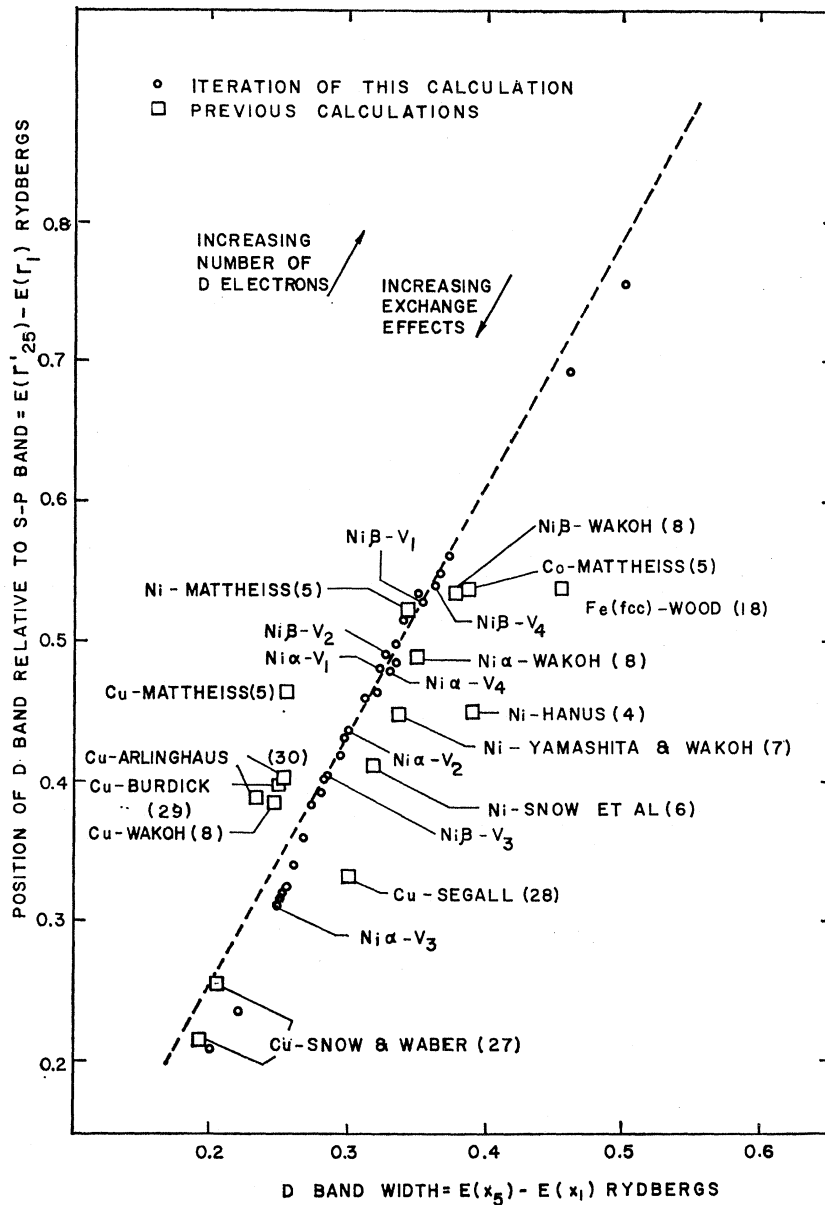


Fig. 4. Comparison of fcc energy band calculations. The bracketed numbers refer to references in the text.

upward from those of Snow and Waber by approximately 0.15 Ry. This is almost exactly the same as the displacement between Wakoh's bands for ferromagnetic Ni and those of V_3 (the self-consistent bands for \bar{V}_x^{fe}). The reason for this discrepancy lies in the simplified version of self-consistency used by Wakoh. The wave functions used to generate a new potential after each iteration were *not* chosen uniformly over the Brillouin zone. His procedure was to pick out 5 functions representative of the d -like electrons (corresponding to local maxima in the density of states curve) and another function representing a conduction electron, corresponding to energy $E(\Gamma_1) + (\frac{3}{5})E_f$. These functions were then weighted to give 5.0 $d\alpha$ electrons, 4.4 $d\beta$ electrons, and 0.3 conduction electrons

of both spins. For the copper calculation, the corresponding weights were 10 d electrons and one conduction electron. Since the "conduction electron" function chosen here is a mixture of s and d -like functions, this procedure tends to fix the amount of d -like character at too high a value, thus displacing the d -bands upward. His final result is very close to that of V_4 (the self-consistent bands for $\frac{2}{3}\bar{V}_x^{fe}$), since the effect of overestimating the exchange tends to balance the effect of using too many d electrons.

C. Comparison with Experimental Data

Of the wealth of experimental data that has been published on nickel, there are several firmly established

facts which should be explained by an energy-band calculation, if the model is to have any validity at all: (1) the saturation value of the magnetization, (2) the electronic specific heat at low temperatures, (3) the Fermi surface topology as deduced from de Haas-van Alphen measurements, (4) the saturation of the magnetoresistance, and (5) the negative spin density found from neutron diffraction and positron annihilation data.

In order to interpret the first two of these properties, we need to calculate from the energy bands, *the density of states*, i.e., the number of allowed energy levels per unit energy. Mathematically this is

$$n_s(\varepsilon) = \frac{\Omega}{(2\pi)^3} \frac{d}{d\varepsilon} \int_{E_s(\mathbf{k}) < \varepsilon} d\mathbf{k},$$

where $E_s(\mathbf{k})$ is the energy of an electron with spin s and reduced wave vector \mathbf{k} and is the volume of the unit cell. Since $E_s(\mathbf{k})$ is not known analytically from the computation, we approximate by

$$n_s(\varepsilon) \simeq (\Delta\varepsilon)^{-1} \sum_{\varepsilon \leq E_s(\mathbf{k}) \leq \varepsilon + \Delta\varepsilon} w(\mathbf{k}),$$

where the sum is over those \mathbf{k} points at which $E_s(\mathbf{k})$ is known, and $w(\mathbf{k})$ is the weight for \mathbf{k} . In this calculation $E_s(\mathbf{k})$ was calculated at only 20 nonequivalent points, which is not enough to give an accurate $n_s(E)$. Using Hodge's interpolation scheme, it was found that evaluating the energies at the 505 points of Grid No. 4 of Table I was sufficient to give a density-of-states

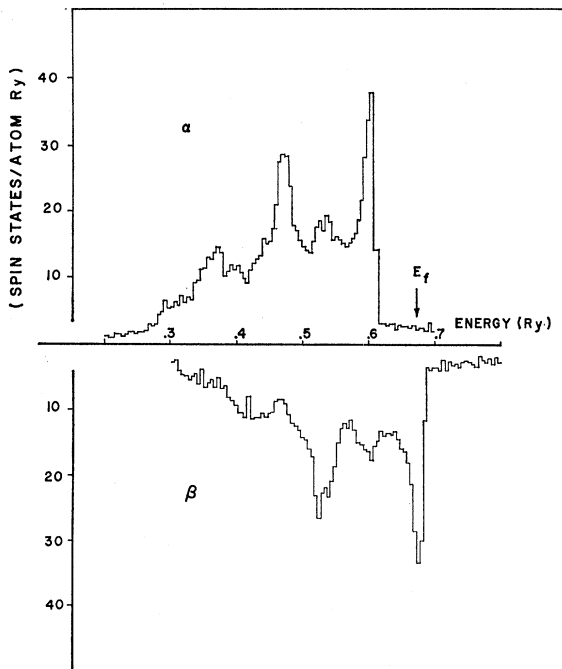


FIG. 5. Density of states for both spins, derived from the interpolated energy bands corresponding to V_4 . The energy is measured with respect to the intersphere potential for the α -spin electrons.

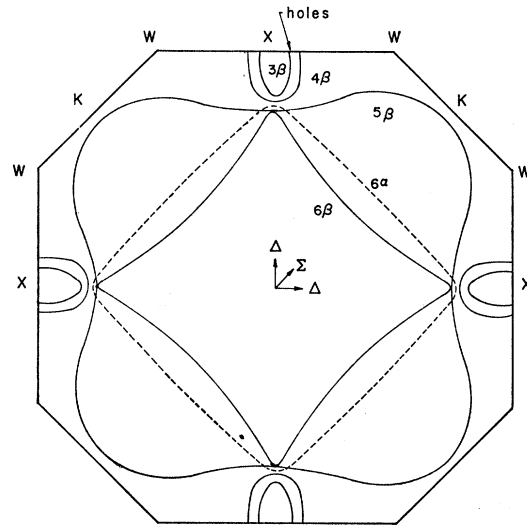


FIG. 6. Cross section of the Fermi surfaces in the $k_x=0$ plane for V_4 . The β -spin surfaces are shown as solid lines and the α -spin surface as a dashed line.

curve with the proper "peaky" nature, shown for V_4 in Fig. 5.

The electronic specific heat c_v at low temperatures is related to the density of states at the Fermi energy by the equation

$$c_v = \frac{1}{3} (\pi^2 k^2) [n_\alpha(E_f) + n_\beta(E_f)].$$

The measured value of c_v corresponds to a total density of 3.1 electrons/atom eV.³¹ The calculated values of $n(E_f)$ are $n(V_3) \sim 4.3$, $n(V_4) \sim 2.7$ electrons/atom eV. The discrepancy in the value for V_3 is a further indictment of these bands, since the method of calculating $n(E)$ should be expected to give a density *lower* than the exact result.

Both calculations show the Fermi energy occurring at a high peak of the density-of-states curve which agrees with Slater's criterion³² for ferromagnetism. The results are also confirmed by the recent measurements of the magnetic susceptibility³³ χ_d , which satisfies a relationship of the form

$$\chi_d^{-1} \propto [n_\alpha(E_f)]^{-1} + [n_\beta(E_f)]^{-1}.$$

The measurements indicate a very small χ_d , which would be obtained only if $n_\alpha(E_f)$ is small. We note that in both V_3 and V_4 , since the α d bands are filled, $n_\alpha(E_f) \ll n_\beta(E_f)$.

Although the Fermi surface of nickel is not as completely mapped out as that of Cu and the noble metals, at least one feature has been firmly established. The de Haas-van Alphen measurements³⁴ indicate a small cross-sectional area of the Fermi surface in the [111]

³¹ W. H. Keesom and C. W. Clark, *Physica* **2**, 513 (1935).

³² J. C. Slater, *Phys. Rev.* **49**, 537 (1936).

³³ A. J. Freeman, reported at the Sanibel Island Symposium in Quantum Theory, January, 1966 (unpublished).

³⁴ A. S. Joseph and A. C. Thorsen, *Phys. Rev. Letters* **11**, 554 (1963).

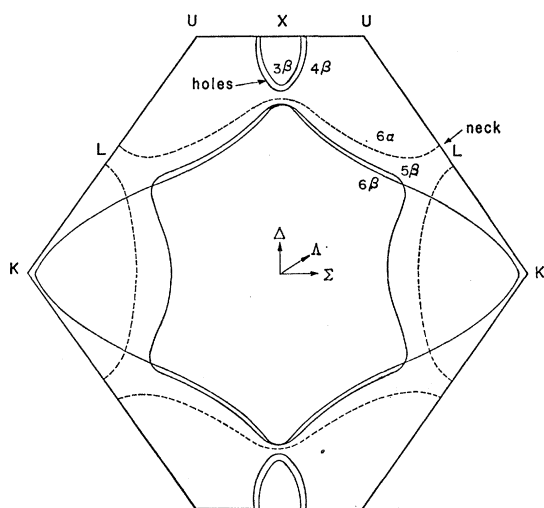


FIG. 7. Cross section of the Fermi surfaces in the $k_x = k_y$ plane for V_4 .

direction. This is interpreted as a "neck" in a Fermi surface similar to that found in copper, i.e., roughly spherical with protrusions that make contact with the Brillouin zone at the L points. The neck area is about $\frac{1}{10}$ that found in Cu, corresponding to an angle of $6.8^\circ \pm 0.2^\circ$ subtended at the Γ point.

The Fermi surface derived from the energy bands for V_4 is shown in two cross sections in Figs. 6 and 7. It consists in this case of four sheets for the down-spin (β) bands and one in the up-spin (α) bands. The β sheets consist of small hole surfaces at the X points in the 3rd and 4th bands, a closed surface with protrusions along the Σ directions in the 5th band, and closed surface with protrusions along the Λ directions in the 6th band. The sole α sheet is a multiply connected surface with necks at the L points, in qualitative agreement with experiment. The calculated angle subtended at Γ is 7.5° , slightly larger than the measured value.

Wakoh's conclusion⁸ that the position of the $L_2'\beta$ level below E_f implies that the 6β Fermi surface be multiply connected is erroneous, as can be seen from Fig. 3.

The model of the α Fermi surface is consistent with the magnetoresistance data of Fawcett and Reed.³⁵ These measurements also show that the magnetoresistance saturates at high magnetic fields. This type of behavior is usually associated with an uncompensated material. Nickel, being an even-valenced metal, would ordinarily be expected to behave like a compensated material. This would be the case in the ordinary energy-band model in which the two spins are degenerate. However, the unrestricted case can give rise to the situation where a different number of bands are occupied for either spin, the sum of the occupation numbers being an odd number. Experimentally,³⁵ the number of electrons per atom must satisfy the relation

$$n_e(\alpha) + n_e(\beta) - n_h(\alpha) - n_h(\beta) = 1.0,$$

³⁵ E. Fawcett and W. A. Reed, Phys. Rev. **131**, 2463 (1963).

where $n_e(s)$ is the number of electrons/atom on the electron Fermi surfaces, and $n_h(s)$ is that on the hole Fermi surfaces. This equation is satisfied by both of the energy bands V_3 and V_4 , since in both cases five of the α bands and four of the β bands are filled, so that only one of the ten valence electrons is left to be distributed over the Fermi surfaces.

Further de Haas-van Alphen measurements³⁶ appear to have found the 4β section of the Fermi surface (the light mass hole pocket at the X point). No evidence was found for the 3β surface, perhaps because of its larger effective mass. However, it should be noted that this feature of the calculated Fermi surfaces is the most doubtful, since a shift upwards of E_f of about 0.005 Ry with respect to the d bands would cause this hole pocket to disappear.

Recently, it has been discovered through measurements of positron annihilation³⁷ and neutron diffraction³⁸ in ferromagnetic Ni, that the electron spin density is negative in the outer regions of the unit cell. It is found that for both V_3 and V_4 , the conduction electrons are polarized opposite to the d electrons, so there is a theoretical negative spin density outside the spheres, and just inside the spheres. The measured³⁸ value of 19% of the magneton number (0.606) is larger than the theoretical ones for both calculations, perhaps because of the neglect of the nonspherical terms of the potential.

TABLE IV. Comparison of calculated and experimental quantities.

Measured quantity	Calculated		Experimental
	V_3	V_4	
Magneton number (Bohr magnetons)	0.65	0.62	0.606
Density of states at the Fermi level (electrons/atom eV)	4.3	2.7	3.1
Neck of 6α Fermi surface, Angle subtended at Γ	...	7.5°	6.8°
Cross-sectional area (atomic units)	...	0.010	0.008
Effective masses (in units of the electron mass) ^a	m_t	...	0.2
	m_l	...	0.5
4β hole surface around the X point			
Cross-sectional areas ^b (atomic units)	0.058	0.072	0.063
	0.023	0.030	0.026
Negative spin density (percentage of the magneton number)	7.8%	9.4%	19%

^a m_t and m_l are the transverse and longitudinal effective masses as defined in Ref. 34.

^b These are the cross-sectional areas parallel and perpendicular to the ΓXU plane.

³⁶ D. C. Tsui and R. W. Stark, Phys. Rev. Letters **17**, 831 (1966).

³⁷ V. L. Sedov, Zh. Eksperim. i Teor. Fiz **48**, 1200 (1964) [English transl.: Soviet Phys.—JETP **21**, 800 (1965)].

³⁸ H. Mook and C. G. Shull, J. Appl. Phys. **37**, 1037 (1966).

A summary of the experimental and calculated data is shown in Table IV. It can be seen that the V_4 self-consistent bands ($V_x = \frac{2}{3}\bar{V}_x^{fe}$) are in much better agreement than those for V_3 ($V_x = \bar{V}_x^{fe}$).

IV. CONCLUSIONS

The purpose of this work has been to solve as accurately as possible within the limits of present computational techniques, the unrestricted Hartree-Fock (UHF) equations in a ferromagnetic solid.

In attempting to solve the UHF equations, we have used the one-electron approximation. This has had considerable success for atomic systems, and it can be shown³⁹ that it can give a solution that is very nearly as good as the exact Hartree-Fock value. There is no reason to believe that the same should not be true for a solid. The problem here is to find the "best" one-electron approximation, i.e., to find an effective local exchange potential that can accurately reproduce the exact Hartree-Fock solution. One way to do this would be to calculate the total energy of the solid in the correct way, viz., $E_t = \langle \Psi | \mathcal{H} | \Psi \rangle$, where Ψ is a determinant made up of the approximate self-consistent one-electron functions and \mathcal{H} is the exact Hamiltonian, and then to minimize E_t with respect to the exchange approximation. Lindgren⁴⁰ has found that this method works very well for atoms, giving *better* agreement with the experimental binding energies than the exact Hartree-Fock method. Such a scheme is of course much more difficult in a solid, but de Cicco¹⁴ has recently shown that it is feasible to compute the total energy of a solid, so that an investigation of this type might be possible in the future.

This has not been done in this work, but it has been shown that slightly changing the one-electron Hamiltonian critically changes the resulting energy-band structure. In particular, it turns out that using the averaged free-electron exchange approximation $\bar{V}_x^{fe} = -6(6\rho_s/8\pi)^{1/3}$ gives qualitative disagreement with experiment, whereas reducing the exchange to $(\frac{2}{3})\bar{V}_x^{fe}$ gives agreement for most of the experimental data. The strongest argument for this conclusion is the Fermi surface structure deduced from the calculated energy bands. The existence of a copper-like Fermi surface with a small "neck" in the $\Lambda[111]$ direction, which has been firmly established^{34,35} by de Haas-van Alphen and magnetoresistance experiments, is *not* predicted by the \bar{V}_x^{fe} bands, but *does* occur when the exchange is reduced. This tends to confirm the conclusion that others have reached for atomic systems, i.e., that \bar{V}_x^{fe} overestimates the exchange effects.

This sensitivity of energy bands to changes in the one-electron approximation was not pointed out in previous calculations of this type, mainly because they were not carried out to self-consistency, and therefore no conclusions could be made about the adequacy of

the Hamiltonian. There *has* been one other calculation for a metal (that of Snow and Waber²⁷ on Cu) that was self-consistent using the \bar{V}_x^{fe} exchange. The discrepancy of the Fermi surface did not occur in this case, since the position of the Fermi level with respect to the position of the d bands is different for Cu than for Ni. In Cu, there are 11 valence electrons per atom, 10 of which are " d like," so that the d bands are full. The Fermi level therefore lies *above* the d bands in Cu, whereas in Ni, having one less valence electron, has its Fermi level slightly below the top of the d bands. In both cases (this work and Ref. 27), going to self-consistency lowers the d bands with respect to the conduction bands. For Cu, the position of E_f with respect to the conduction bands remains essentially the same, but for Ni, E_f is lowered with respect to the conduction bands. The position of E_f with respect to the conduction bands is what determines the shape of the Fermi surfaces. Therefore, going to self-consistency in Cu showed no qualitative change in the Fermi surface, as is the case for Ni.

Actually, before we can definitely say whether the discrepancy is due to the inaccuracy of \bar{V}_x^{fe} , we should examine the approximations made in this computation, in order to see if there could possibly be some effect which would shift the bands enough to bring the \bar{V}_x^{fe} bands into agreement with experiment. From Fig. 32, it can be seen that this shift would have to be approximately 0.1 Ry in order to bring the d bands up far enough to give the experimentally observed Fermi surface.

There are four important approximations which have been used in this computation:

A. Neglect of Relativistic Effects

They can be handled within the framework of the energy-band model, and are certainly important for heavy atoms. Calculations which have been made (e.g., Ref. 41) show that these effects are on the same order of magnitude in a solid as in a free atom. For the Ni atom, the relativistic splittings of the one-electron energy values are¹² ~ 0.01 Ry, so that it does not appear that they could qualitatively change the Fermi surface structure.

B. Neglect of the Nonspherical Component of the Potential

In deriving the potential of Eq. (9) from a muffin-tin charge density we used the spherical average instead of the actual Ewald potential. In Ref. 15, it is shown how these effects can be taken into account, by expanding the non-muffin-tin part of the potential in terms of a Fourier series. For example, it turns out that the L_2' level can be well approximated by a single symmetrized plane wave corresponding to $\mathbf{k} = (\pi/a)[111]$. The

³⁹ I. Lindgren, Phys. Letters **19**, 382 (1965).

⁴⁰ I. Lindgren, Arkiv Fysik **31**, 59 (1965).

⁴¹ J. B. Conklin, L. E. Johnson, and G. W. Pratt, Phys. Rev. **137**, A1282 (1965).

Fourier component of the Ewald potential corresponding to $\mathbf{K} = (2\pi/a) [111]$ is¹⁵ equal to $-(Q/a)$ (0.0096). Substituting in values of $Q=0.26$ and $a=6.65$ shows that the energy shift of the L_2' level would be on the order of only 0.001 Ry. Since this level is the one which determines the neck of the Fermi surface, it appears that the inclusion of these non-muffin-tin terms would change the resultant Fermi surface only by a negligible amount.

C. Neglect of the Nonspherical Components of the Charge Density

The Ewald potential was derived on the assumption of a muffin-tin charge density. However, the departures of the actual density from this approximation are certainly significant, as can be seen from the neutron-diffraction data. These effects are much harder to estimate,¹⁴ especially the nonspherical parts within the spheres. It can be done by an expansion in terms of spherical harmonics, but if more than a few l values are important, the number of integrals to be calculated becomes prohibitively large. They should, of course, be investigated if the data are to be accurately interpreted, but it is unlikely that they will seriously affect the energy-band structure as presented here.

D. Neglect of the Distortion of the Core States

In this calculation, the core-state wave functions ($1s$, $2s$, $2p$, $3s$, and $3p$) were assumed to remain unchanged from the values found for the Ni atom. Snow and Waber²⁷ in their calculation on Cu tried to estimate the error involved in this assumption. They used two values of the core density, one obtained from an ordinary self-consistent atomic calculation, and the other, from an atomic calculation in which all of the wave functions were constrained to be in the Wigner-Seitz sphere (i.e., that sphere with volume equal to a unit cell). It was found that constraining the core states had the effect of pushing the d states *up* with respect to the conduction band by approximately 0.03 Ry. During the course of this work, the bands corresponding to the $3s$ and $3p$ levels were computed using the actual crystalline potential, and a new potential derived from the resultant wave functions. The changed potential

shifted the d bands up by an amount less than 0.01 Ry. Neither estimate is enough to qualitatively change the Fermi surfaces, although a more accurate calculation should certainly take the distortion of the core states into account.

The arguments presented here, although not conclusive, tend to suggest that any discrepancy found can be attributed to the approximation made in the Hamiltonian, rather than in the approximations made to find the eigenvalues of this Hamiltonian.

To this list of approximations another could possibly be added, i.e., the neglect of any correlation effects. These are of course not included in the Hartree-Fock model, but they may be important in ferromagnetic nickel. However, the importance of correlation cannot be determined if the exchange is not known accurately. Indeed, it may be that the averaged free-electron approximation is a better estimate of the Hartree-Fock exchange effects than it appears here, and that reducing the magnitude of the exchange merely introduces some effective correlation. More study is needed on these effects, if the energy-band model is to be successful in the explanation of ferromagnetic effects.

In conclusion, the main result of this work is that the unrestricted Hartree-Fock equations can be solved in a solid, at least in one-electron model, and that this scheme forms a reasonable model for a ferromagnetic solid. The accuracy obtained is sufficient to give at least qualitative agreement with experiment, and could probably be improved if better approximations to the Hamiltonian were used.

ACKNOWLEDGMENTS

I would like to acknowledge the help offered by Professor J. C. Slater, who suggested the problem upon which this paper is based. Thanks are due to many members of the Quantum Theory Project at the University of Florida, including Dr. S. O. Goscinski and Dr. K. H. Johnson for many piquant discussions, and especially to Dr. J. B. Conklin for his assistance with the computer programs. I would also like to express my appreciation to Dr. J. H. Wood for providing several computer programs, and to the University of Florida Computing Centre for the use of their facilities.